

# Soft probes of high density QCD physics with CMS

Ferenc Siklér for the CMS Collaboration

KFKI Research Institute for Particle and Nuclear Physics, Budapest, Hungary

E-mail: sikler@rmki.kfki.hu

**Abstract.** The CMS heavy-ion program will probe QCD matter under extreme conditions. Its capabilities for the study of global observables and soft probes are described.

## 1. Introduction

The CMS experiment at the LHC is a general purpose detector designed to explore physics at the TeV energy scale. It has a large acceptance and hermetic coverage. The various subdetectors are: a silicon tracker with pixels and strips ( $|\eta| < 2.4$ ); electromagnetic ( $|\eta| < 3$ ) and hadronic ( $|\eta| < 5$ ) calorimeters; and muon chambers ( $|\eta| < 2.4$ ). The acceptance is further extended with forward detectors: CASTOR ( $5.3 < |\eta| < 6.6$ ) and Zero Degree Calorimeters ( $|\eta| > 8.3$ ). CMS detects leptons and both charged and neutral hadrons. In the following the CMS soft physics capabilities are described. For a recent extensive review see Ref. 1.

## 2. Soft physics

### 2.1. Minimum bias trigger

To maximize efficiency, it is desirable to trigger on regions with a large number of produced particles. The level-1 trigger read-out will utilize hadronic cells, towers. In order to reject non-collision events, such as those due to beam-gas collisions, the interaction trigger could require a coincidence of signals from both hadronic forward (HF) calorimeters. The rejection of such spurious events would not be achievable using only the central calorimeter as a trigger. At the same time, this choice would reduce the efficiency for single diffractive processes.

The p-p trigger will be based on counting towers with energy above the detector noise level, in both forward hadronic calorimeters ( $3 < |\eta| < 5$ ). A minimal number of hits (1, 2 or 3) will be required on one or on both sides. The trigger efficiency for different total number of particles using several symmetric settings is shown in Fig. 1-left, where a threshold value of 1.4 GeV was used. In case of higher luminosity, events with random trigger could also be taken, because overlapping events can also be reconstructed.

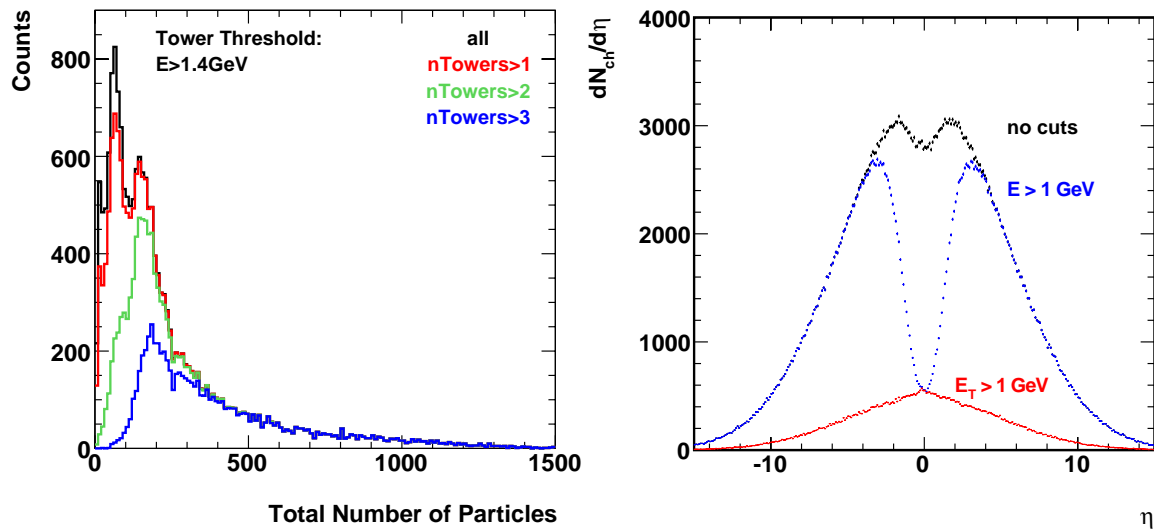


**Figure 1.** Left: Estimated loss of low multiplicity events due to triggering requirements on the number of towers for cuts on  $E$  in minimum bias p-p collisions at 14 TeV. Right: Pseudorapidity distribution of charged hadrons in central Pb-Pb collisions at 5.5 TeV per nucleon from the HYDJET [2] generator. Particle selection to mimic the level-1 trigger is applied for total  $\langle E \rangle$  and transverse  $\langle E_T \rangle$  energy.

The Pb-Pb trigger will be similar since there are many particles produced in the region of the forward calorimeters (Fig. 1-right). Although triggering will be possible for the most central collisions with transverse energy cuts ( $E_T$ ), more peripheral collisions with lower multiplicity will suffer from inefficiency. For total energy cuts ( $E$ ), only events with  $b > 12$  fm suffer from inefficiency, relative to the p-p baseline.

## 2.2. Centrality determination

In CMS, a simple method of determining the impact parameter on an event-by-event basis is to use the transverse energy deposited in the calorimeters, which decreases strongly from central to peripheral collisions. Due to its relatively low initial parton density, the very forward rapidity region covered by the HF and CASTOR calorimeters,  $|\eta| > 3$ , is expected to be nearly free of final-state rescattering compared to the central rapidity region. Therefore the energy deposition is determined mainly by the initial nuclear geometry of the collision rather than by final-state dynamics (Fig. 2-left). Using the forward spectator neutron energy measured in both zero degree calorimeters can improve the experimental impact parameter resolution of a few tenths of a fermi.

## 2.3. Charged particle multiplicity

It is possible to measure the rapidity density and multiplicity of produced charged particles event-by-event. The technique is based on the relation between the pseudorapidity distribution of reconstructed hit clusters in the innermost layer of the pixel tracker and that of charged particle tracks originating from the primary vertex.

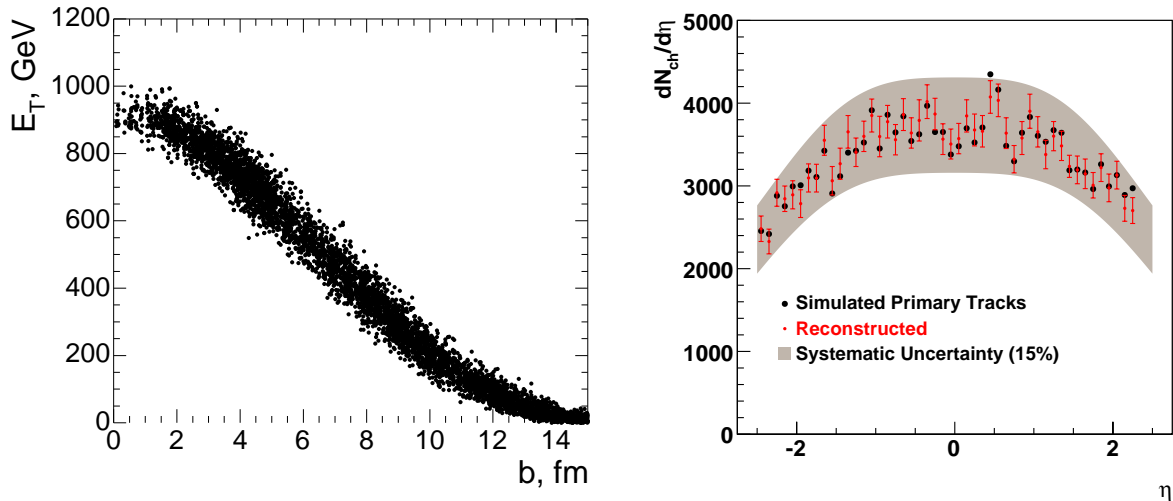


**Figure 2.** Left: Correlation between the impact parameter,  $b$ , and the transverse energy,  $E_T$ , deposited in the forward rapidities,  $5.3 < |\eta| < 6.6$ , covered by the CASTOR calorimeter, as simulated with HIJING for 3000 minimum bias Pb-Pb collisions. Right: Comparison of the original distribution of primary simulated tracks (large points) to the estimate obtained from the reconstructed hits in the innermost pixel layer (smaller points with statistical error bars).

Corrections are needed for hits from non-primary sources: looping particles in magnetic field, secondaries and noise. Because the amount of energy deposited is proportional to the length traversed in the silicon, charged particle tracks with longer path lengths will deposit more energy. This observation is a powerful method for eliminating most non-primary hits. A cut in  $\cosh \eta$  selects only hits where the energy deposition is consistent with particles emanating from the true collision vertex. Based on previous measurements and recent studies, an accuracy of about 2% is expected with systematic errors below 10% [1] (Fig. 2-right).

#### 2.4. Low $p_T$ tracking

In CMS, the measurement of charged particle trajectories is achieved primarily using the silicon tracker with both pixels and strips, embedded in a 4 T magnetic field. The high granularity silicon pixel tracker consists of three barrel layers (at about 4, 7 and 11 cm radius) and two endcap disks. There are about 66 million pixels with an area of  $100 \times 150 \mu\text{m}^2$ . The strip part is a combination of single- and double-sided layers with ten barrel and nine forward layers on each side (9.3 million channels). The reconstruction capabilities at lower  $p_T$  are limited by the high magnetic field and effects of the detector material. In addition, in central Pb-Pb collisions the high occupancy of the silicon strips makes the inclusion of these strips in charged particle tracking difficult.

The track finding procedure, modified for low  $p_T$ , starts by pairing two hits from different layers. During the search for the third hit, the following requirements must be fulfilled: the track must come from the vicinity of the beam-line; the  $p_T$  of the track must

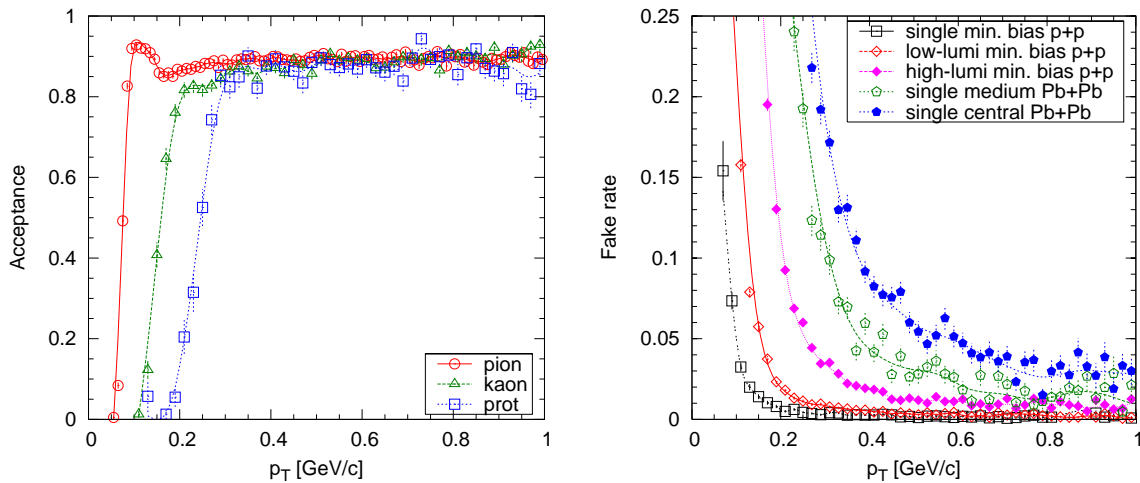


**Figure 3.** Left: Acceptance of the track reconstruction algorithm as a function of  $p_T$  for tracks with  $|\eta| < 1$ . Values are given separately for pions (circles), kaons (triangles) and (anti)protons (squares). Right: Reconstruction rate of fake tracks as a function of  $p_T$ , for tracks with  $|\eta| < 1$ , for single, low luminosity and high luminosity minimum bias p-p events and for central and mid-central Pb-Pb collisions.

be above the minimal value  $p_{T,\min}$ ; and the track must be able to reach the layer where the third hit may be located. In the small volume of the pixel detector the magnetic field is practically constant and the charged particles propagate on helices. The projection of a helix or a cylinder onto the transverse plane is a circle. Each requirement defines a region of allowed track trajectories. They are enclosed by a pair of limiting circles which can be constructed using simple geometrical transformations. A third hit candidate is accepted if its position is within a region which takes into account the expected multiple scattering.

While high  $p_T$  tracks are relatively clean, uncorrelated hit clusters can often be combined to form fake low  $p_T$  tracks. A hit cluster contains more information than just its position. Its geometrical shape depends on the angle of incidence of the particle: large angles will result in longer clusters. We can thus check whether the measured shape of the cluster is compatible with the predicted angle of incidence of the track: if any of the hits in the triplet is not compatible, the triplet is removed from the list of track candidates.

Using this modified pixel hit triplet finding algorithm, charged particles down to very low  $p_T$  can be reconstructed (Fig. 3-left). The acceptance and efficiency is at 80–90%, while the  $p_T$  resolution is about 6%. At the same time a low fake track rate is achieved thanks to the geometrical shape of the hit cluster. It is below 10% even in central Pb-Pb collisions for  $p_T > 0.4$  GeV/c (Fig. 3-right). It is possible to study identified particle spectra (down to  $p_T$  of 0.1 – 0.3 GeV/c) and yields, multiplicity distributions and correlations [1].

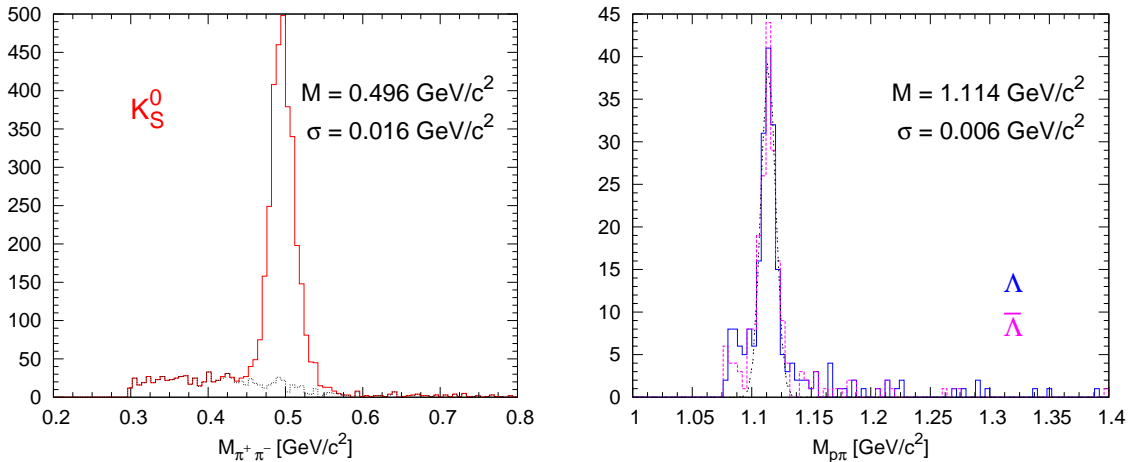


**Figure 4.** Left: Invariant mass distribution of reconstructed  $K_S^0 \rightarrow \pi^+\pi^-$  in single minimum bias p-p collisions. The mass distribution of the background is indicated with a dashed histogram. Right: Invariant mass distribution of reconstructed  $\Lambda \rightarrow p + \pi^+$  and  $\bar{\Lambda} \rightarrow \bar{p} + \pi^-$  in single minimum bias p-p collisions with  $dE/dx$  selection for the secondary proton or antiproton.

### 2.5. Identified particles

Particles can be identified by decay topology and by energy loss measurements in the silicon (in the range  $p < 1 - 2$  GeV/c, benefitting from analogue readout). Weakly-decaying neutral particles have a sizeable probability to decay far from the primary event vertex. Likewise, the silicon detectors can be used to reconstruct photons through their conversion to  $e^+e^-$  pairs in the material of the beam-pipe, silicon pixels and supports. The search for V0 candidates is reduced to determining the closest distance between two track helices. The  $K_S^0$  is reconstructed with a resolution of 16 MeV/c<sup>2</sup> and an average mass of 0.496 GeV/c<sup>2</sup> (Fig. 4-left). The  $\Lambda$  and  $\bar{\Lambda}$  peaks are located at 1.114 GeV/c<sup>2</sup> with a 6 MeV/c<sup>2</sup> resolution (Fig. 4-right). The proton signal was strongly enhanced by a cut on the truncated mean of their  $dE/dx$ , removing almost all the background. In the case of single collisions or low luminosity p-p running, the resonances can be exclusively identified. For high luminosity p-p running or Pb-Pb collisions, the inclusive yield can still be extracted. Multi-strange baryons ( $\Xi^-$ ,  $\Omega^-$ ), open charm ( $D^0$ ,  $D^{*+}$ ) and open beauty ( $B \rightarrow J/\psi + K$ ) can also be studied.

### 2.6. Elliptic flow

The reaction plane in Pb-Pb collisions can be reconstructed using electromagnetic and hadronic calorimeters, by extracting harmonic angular coefficients of the energy deposition distribution  $dE/d\varphi$  (Fig. 5-left). The calculated event plane resolution as a function of impact parameter is shown in Fig. 5-right. The interplay of multiplicity and anisotropic flow in opposite centrality directions gives the best resolution in semi-central

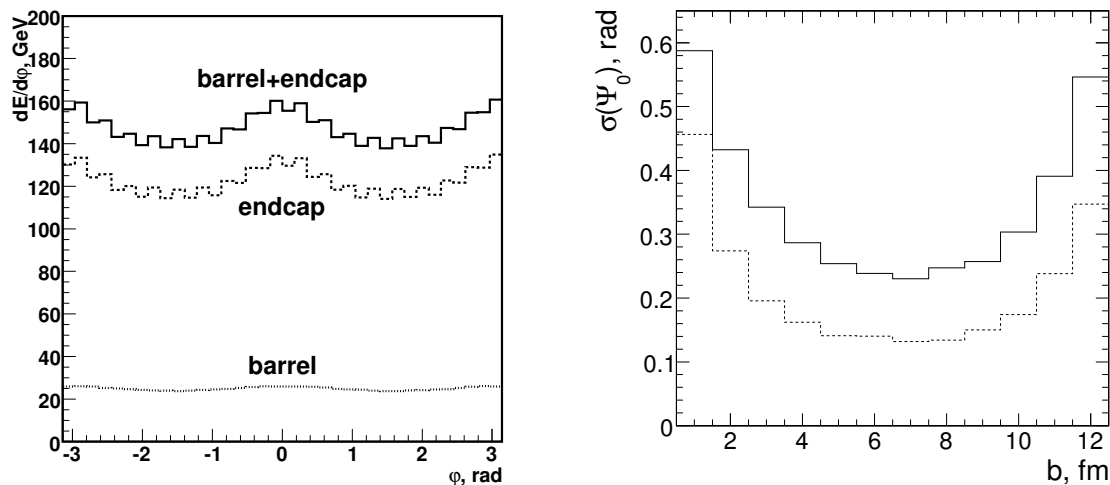


**Figure 5.** Left: Azimuthal dependence of the total energy deposition in the CMS calorimeters in Pb-Pb collisions at  $b = 9$  fm (solid histogram). The barrel and endcap regions are shown separately. Right: Resolution of the event plane angle  $\Psi_0$ ,  $\sigma(\Psi_0)$ , as a function of impact parameter in Pb-Pb collisions with total particle multiplicities  $N_0$  ( $b = 0$  fm) = 58 000 (solid histogram) and 84 000 (dashed histogram).

collisions. The results will improve by adding tracker information and using forward detectors such as the zero degree calorimeter. The second harmonic coefficient  $v_2$  can also be determined using the two-particle azimuthal correlator, without the event plane angle. The advantage of this method is that it automatically corrects for the detector anisotropies.

### 3. Summary

The CMS detector has a good capability for global event characterization and physics with soft probes. The performance in minimum bias triggering, centrality determination, measurement of charged particle multiplicity, low  $p_T$  tracking, particle identification and measurement of elliptic flow has been shown.

### Acknowledgment

The author wishes to thank to the Hungarian Scientific Research Fund (T 048898).

### References

- [1] D. d’Enterria *et al.*, J. Phys. G **34**, 2307 (2007).
- [2] I. P. Lokhtin and A. M. Snigirev, Eur. Phys. J. C **45** (2006) 211 [arXiv:hep-ph/0506189].